Journal of
Composites Science

MDPI

Review

Characterization of Agricultural and Food Processing Residues for Potential Rubber Filler Applications

Cindy S. Barrera [1,*] and Katrina Cornish [2,3]

[1] Research and Advanced Engineering, Ford Motor Company, Dearborn, MI 48124, USA
[2] Food, Agricultural and Biological Engineering, Ohio Agricultural Research and Development Center, College of Food, Agricultural and Environmental Sciences, The Ohio State University, Wooster, OH 44691, USA; cornish.19@osu.edu
[3] Horticulture and Crop Science, Ohio Agricultural Research and Development Center, College of Food, Agricultural and Environmental Sciences, The Ohio State University, Wooster, OH 44691, USA
* Correspondence: cbarre61@ford.com; Tel.: +1-313-845-5559

Received: 28 October 2019; Accepted: 21 November 2019; Published: 26 November 2019

Abstract: Large volumes of agricultural and food processing residues are generated daily around the world. Despite the various potential uses reported for this biomass, most are still treated as waste that requires disposal and negatively impacts the environmental footprint of the primary production process. Increasing attention has been paid toward the use of these residues as alternative fillers for rubber and other large-scale commodity polymers to reduce dependence on petroleum. Nevertheless, characterization of these alternative fillers is required to define compatibility with the specific polymer, identify filler limitations, understand the properties of the resulting composites, and modify the materials to enable the engineering of composites to exploit all the potential advantages of these residue-derived fillers.

Keywords: filler characterization; sustainable filler; renewable composites; added value

1. Introduction

Valorization of agricultural and food processing residues is not only an environmental trend nowadays, but also an important economic goal. These residues represent a widely and continuously available source of renewable raw materials. However, most of them lack a valuable application and are treated as wastes that require costly disposal and have large negative environmental impacts. These waste streams have been considered as potential sources of high-value chemicals, biomass for energy production and animal feed [1–3], but utility depends on particular chemical composition and the economic feasibility of the extraction and transformation processes. In practice, the consumption of agricultural and food residues is still very low. By 2050, we will need to generate 60–70% more food than is currently produced to feed the expected population of more than 9 billion people, by combining increased production with reduced loss and waste [4]. This implies a concomitant increase in already abundant crop and processing residues. Hence, diversified applications of the vast amounts of agricultural and food processing residues daily generated worldwide are required to consume these poorly exploited resources effectively.

In the last two decades, increasing research has focused on the use of agricultural and food processing residues as alternative sources of fillers for rubber composites. This area of research is driven by the need to decrease dependence on petroleum derivatives, concerns about environmental footprint and sustainability of the rubber industry and the need to secure long-term, high volume, supplies of raw materials. Composites consist of two or more primary materials combined to produce one material with properties not possessed by the individual constituents [5]. Some agricultural and

food processing residues studied for the manufacture of rubber composites are fibers, such as oil palm fiber, bananas and coir fibers [6–8], and other highly abundant residues, such as rice husks, processing tomato peels, cuttlebone, eggshells, soy hulls and other soy byproducts [9–14].

Fillers are the second most important component of rubber composites by volume used. These polymer additives are commonly used either as diluents, process improvers, aesthetic improvers, or reinforcers [15–17]. Diluent fillers reduce the cost of rubber products by reducing the more expensive polymeric matrix proportion. During processing, fillers can improve extrudability and reduce power consumption. Fillers can confer or enhance desirable qualitative characteristics, such as texture and color. Material reinforcement is the most important functionality of fillers, and most industrial applications of elastomers would not be possible without reinforcing fillers. In general, filler reinforcement of rubber enhances properties, such as modulus, tensile and tear strength, abrasion resistance, hardness and stiffness [18–20]. In unfilled products, properties like fatigue resistance, tensile and tear strength, and toughness reach a maximum value at an optimal polymer network crosslink density, and additional crosslinking leads to decreases in these properties [21,22]. Reinforcing fillers are used to enhance these properties beyond the values achieved by optimal crosslink density alone.

Currently, the main reinforcing filler for rubber is carbon black, a petroleum-derived nanofiller. Consumption of this material reached 11.8 million metric tons in 2013 [23], and demand is increasing in parallel with rubber demand. Global rubber consumption has steadily increased over the last 16 years: Total rubber consumption (natural and synthetic) reached 26.73 million metric tons in 2015, a 49% increase compared to 2000, when total consumption was 17.94 million metric tons [24].

Approximately 90% of carbon black production is used in rubber products [25]. Carbon black is a non-renewable filler obtained from the partial combustion or thermal decomposition of fossil fuel-derived hydrocarbons [26,27]. Carbon black production generates large quantities of greenhouse gas pollutants, such as sulfur dioxide, carbon dioxide, nitrogen oxide and particulate matter. Strict environmental regulations placed by the US Environmental Protection Agency for carbon black production in North America, combined with increasing demand, may lead to a shortfall of approximately 210,920 metric ton/year by 2020 and concomitant rising prices [28,29]. Existing non-carbon black fillers include high surface area precipitated silanized silica (another reinforcing filler), calcium carbonate (a diluent, polymer extender filler) and other inorganic materials derived from the grinding or precipitation of minerals, and are neither renewable nor sustainable.

The use of agricultural and food processing residues for rubber composites would have multiple environmental and economic benefits. Economic benefits include reduction of costs associated with residue treatment and disposal, and of the final cost of polymeric products. Environmental gains are achieved by the reduction of greenhouse gases generated by waste decomposition in landfills, and reduced extraction of mineral fillers. Additional advantages of rubber composites made with waste-derived fillers include accelerated composite decomposition after end-of-life disposal and improved sustainability of rubber products [30,31]. Furthermore, many of these residues, i.e., shells, peels and stems, are lightweight natural structural materials possessing good mechanical properties.

Inevitably, there are some drawbacks associated with the use of agricultural and food processing residues. In order to be used as filler, these materials must be ground to small particles and size reduction entails cost. Moreover, most bio-based fillers have lower compatibility than carbon black with non-polar elastomers, like natural rubber, styrene butadiene rubber, polybutadiene rubber and ethylene-propylene rubber, due to their more polar nature [9,32,33]. However, this latter limitation can be overcome by the use of surface functionalization [34–38]. Furthermore, the active surface of these materials, and their complex composition and diverse particle shapes and structures, offer potential tailoring of composite properties to meet specific application requirements, and allow unique and unusual combinations of material properties [10,11].

Agricultural and food processing residues represent a promising, yet not well understood or exploited, source of fillers for rubber composites. Existing rubber reinforcing mechanisms have been defined based on carbon black or silica. Although there are common factors between these conventional

fillers and bio-based fillers that affect rubber reinforcement, characterization of fillers obtained from agricultural and food processing residues is needed to identify other attributes that can impact rubber reinforcement and predict composite performance. In this review, we outline important characteristics to consider when selecting residue-derived fillers and describe characterization methods that can help elucidate their interaction with the rubber matrix and predict and explain composite performance.

2. Filler Characterization

The reinforcement of elastomers by fillers is the result of a combination of physical and chemical interactions [39]. These complex interactions allow material flexibility to be maintained, while enhancing strength and resistance to deformation [16] Morphological and physicochemical properties of fillers determine the type and strength of the interactions between the polymer and the filler and, hence, the final composite properties [16,18,40,41]. In conventional carbon black and silica fillers, which have standardized production methods and very defined chemical composition, the primary filler characteristics that affect material performance are filler surface area, structure and surface activity [18,19]. Although these characteristics also are important for bio-based fillers, they are not the only characteristics that can affect rubber composite performance. Fillers with a wide diversity of particle size, shape, structure, chemical composition and crystallinity can be achieved from agricultural and food processing residues depending on the source of the material and the extraction method used [10,42]. A single method will not provide all the information needed to characterize all the materials, but a combination of multiple techniques selected based on the type of filler, polymer application and processing conditions, can be effective.

2.1. Surface Area

Surface area is arguably the most important morphological characteristic affecting filler reinforcing potential [16,19,43]. This filler characteristic directly impacts its interfacial contact area with the polymer. Larger surface area and higher filler loading (amount of filler in the composites) facilitate more interfacial contact between the filler and the polymer, thus, increasing reinforcing potential [18,40,44]. For conventional, non-renewable fillers, particle size is inversely proportional to particle surface area, and so this parameter is commonly used as a simple classification criterion for conventional fillers (Figure 1).

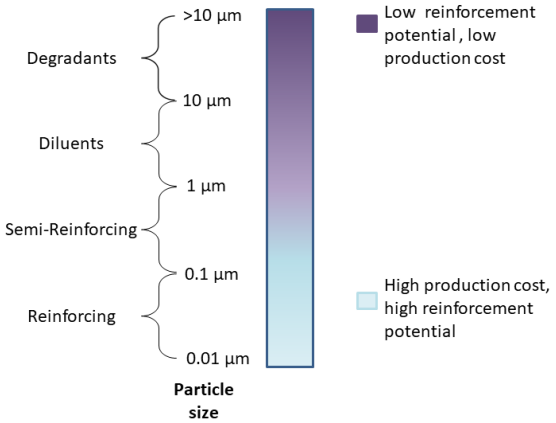

Figure 1. Classification of fillers according to average particle size. Adapted from reference [19].

Based on this classification, reinforcing filler particles have at least one dimension in the nanoscale (<100 nm), and are known as nanoparticles. The superior reinforcement achieved with these small particles compared to larger sized particles, relies on there being greater numbers of particles per volume of rubber, and a greater interfacial contact area [20,44]. Big particles also may act as localized stress-raising inclusions, generating flaws within the composite that can initiate failure [20,40].

Despite the large surface area offered by nanofillers, important limitations have been identified, particularly for non-carbon black nanofillers like those obtained from agricultural and food processing residues. Nanoparticles are often much more expensive to produce than macro and micro size particles, and good filler dispersion within the polymer matrix is challenging [40,45–48]. Depending on the material, extensive hours of milling, harsh chemicals, high temperatures, and high pressures may be required to prepare nanoparticles (Figure 2) [46,49–51]. Furthermore, the higher surface area of nanoparticles increases the attraction between the particles, leading to their agglomeration and reduced composite performance [16,52,53]. To achieve homogeneous dispersion of nanoparticles in the rubber, complex mix protocols are required that often involve high power consumption, increasing processing costs [44,48].

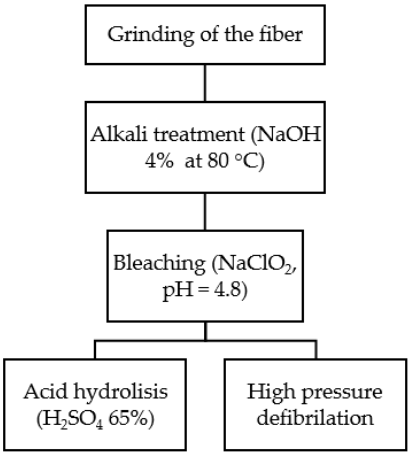

Figure 2. Schematic of main methods for extraction of cellulose nanoparticles. Adapted from references [42,54].

Particle size is not the only characteristic affecting rubber reinforcement by bio-based fillers. Filler surface activity determines the strength and nature of the polymer-filler interaction [41] and structural features, such as material porosity, also play a role in reinforcement and can increase surface area of the filler. Hence, fillers with similar particle size may reinforce differently. Barrera and Cornish [55] identified bio-based rubber composites made with micro sized fillers that have similar or better performance than composites made with a nanosized version of the same material. Moreover, composites made with micro sized fillers had a much lower energy consumption than nanofillers during the mixing of the materials.

Nitrogen, cetyl triethyl ammonium bromide (CTAB) and iodine adsorption, are used to estimate filler surface area [16,40]. However, these methods involve molecular adsorption, which means that results are affected by the surface area and surface activity of the filler. Furthermore, iodine is highly reactive, while CTAB requires calibration curves made using different standard carbon blacks.

Nitrogen Adsorption

Multilayer gas adsorption behavior, based on the Brunner, Emmet and Teller (B.E.T) method, is the most commonly used technique to estimate filler surface area [16]. The B.E.T theory is based on the physical adsorption of gas molecules onto the surface of materials. The amount of gas adsorbed at a constant temperature (adsorption isotherm) is proportional to the surface area in contact with the gas, and is dependent on its relative vapor pressure [56]. Filler surface area is determined from the linear region of the adsorption isotherms of nitrogen given by the B.E.T. equation [57,58]:

$$\frac{P}{V_a(P_O - P)} = \frac{1}{V_m C} + \frac{C-1}{V_m C} \times \frac{P}{P_o} \quad (1)$$

where P is the manometer pressure in kPa, P_o is saturation vapor pressure of nitrogen in kPa, V_a is the volume of nitrogen adsorbed per gram of sample, V_m is the volume of nitrogen per gram that covers one monomolecular layer in standard cm^3/g and C is the B.E.T constant. Its numerical value depends on the heat of adsorption by the monomolecular layer [58].

Although this method is the most widely accepted, it assumes that the filler surface is energetically homogeneous [27], which is rarely the case for bio-based materials. The surface of most bio-based fillers can be highly polar and possess functional groups, exposed ions and a mix of amorphous and crystalline areas. Surface area using nitrogen adsorption is calculated assuming the molecular cross-sectional area of the adsorbate is known. However, due to the quadrupolar nature of nitrogen molecules, interaction of nitrogen with the polar surface of bio-based fillers can change the orientation and micropore filling pressure, which leads to a miscalculation of the true surface area of bio-based fillers [59]. For instance, bio-based fillers evaluated at two different particle sizes showed lower surface area for micro sized cellulosic material than macro sized particles of the same material [60]. This could be due to a decrease in an aspect ratio of the particles or changes in the surface chemistry, due to prolonged grinding. The same study found that particles obtained from different residues with similar particle size distribution showed considerable differences in surface area and pore volume [60].

Other adsorbates like argon, which does not have polar interactions with surface functional groups, may deliver a more accurate measurement. However, interpretation of argon isotherms is not as simple as for nitrogen isotherms. Furthermore, nitrogen is cheaper than argon and, despite the uncertainty of the true surface area of bio-based fillers, nitrogen adsorption surface area has been standardized as a predictive tool of performance of conventional fillers.

In addition to the total surface area, nitrogen absorption also provides information about porosity and surface treatment in bio-based fillers. Micro-pores measured by nitrogen adsorption is not accessible to many rubber polymers, due to their large size, and so they are not considered important for the reinforcing efficiency of carbon black. However, in bio-based fillers, pores in polar particles can contain moisture and other smaller molecules than could negatively affect reinforcement of the rubber and, hence, this is useful information for the characterization of the material. Moreover, these pores can have active sites for coupling agents [61]. Nitrogen absorption by calcium carbonate before and after different levels of surface treatment with stearic acid showed a decrease in the equilibrium concentration as the degree of surface coverage increased [62].

For bio-based fillers, the high surface area can result from materials having broad particle size distribution and complex structure. Thus, particle size analysis using laser diffraction and/or microscopy is recommended to complement the information provided by absorption methods.

2.2. Surface Activity

Filler surface activity reflects the abundance and concentration of high energy sites in the material surface and influences filler dispersibility and filler compatibility within the rubber. This filler characteristic determines the type and strength of the polymer filler interaction, and hence, the degree of composite reinforcement [63,64]. For instance, fillers with high amounts of active surface hydrogen ions, generate strong filler-filler networks that can lead to agglomeration problems during processing and limit the reinforcement efficiency of the filler in most non-polar elastomers. Although high energy sites are mainly associated with functional groups [18,40,65], the surface activity also depends on the accessibility of these sites, which is determined by the arrangement and orientation of surface chemical groups [66,67]. Furthermore, high energy sites also can arise at structural heterogeneities, such as boundaries between crystallites and amorphous regions [19,67,68]. Therefore, highly active filler surfaces can result in a variety of interactions ranging from Van der Waals forces to chemical interactions.

Filler surface activity is measured as surface free energy, a parameter that describes the interactive potential of a given surface [69,70]. Surface free energy (γ_S) of a solid surface is the result of dispersive (γ_S^D) and specific components (γ_S^{SP}) [71,72]:

$$\gamma_S = \gamma_S^D + \gamma_S^{SP}. \quad (2)$$

The dispersive component represents the surface's ability to interact through London type interactions [64,73]. These weak intermolecular forces play the main role in the interaction of fillers with non-polar molecules, such as most general purpose rubbers. In contrast, the specific component represents the interactions, due to all other types, such as acid–base, magnetic, metallic, and hydrogen bonding [74]. Therefore, fillers that have a high specific component and a low dispersive component are associated with weak polymer-filler and strong filler-filler interactions [19].

Surface energy characterization is particularly important for fillers obtained from agricultural and food processing residues. Varied and complex materials composition causes variations in surface energy, as do different feedstock sources and production methods. For instance, milling particles can increase surface energy by disrupting crystalline structures and exposing high energy sites [75]. Moreover, surface energy characterization is required to evaluate the efficiency of filler surface modifications.

Unlike surface area measurement, there are no standardized methods for the quantification of surface energy. Currently, the most commonly used methods are contact angle and inverse gas chromatography [64,73].

2.2.1. Contact Angle

The measurement of liquid–solid contact angle is a commonly used method for the characterization of solid surfaces. The surface energy-dispersive and specific components are obtained from the Young equation [50,72]:

$$Cos\theta + 1 = \frac{2\left(\gamma_s^D \gamma_l^D\right)^{\frac{1}{2}}}{\gamma_l} + \frac{2\left(\gamma_l^{SP} \gamma_l^{SP}\right)^{\frac{1}{2}}}{\gamma_l}, \quad (3)$$

where the superscripts s and l are the surface energy of the solid and the liquid, respectively, and θ is the contact angle.

Although contact angle offers a simple way to characterize solid surfaces, these methods were designed for macroscopically flat surfaces, not for small particles, and are not very effective on particulates, rough surfaces and chemically heterogenous materials, such as those of bio-based fillers [65,76,77]. Despite adaptations like the compression of samples to form planar surfaces and adherence of particles to glass slides or tapes (Figure 3), it is difficult to obtain reliable measurement of surface energy for bio-based fillers, especially when comparing different materials. Attempts to obtain quantitative information of surface energy report high scattering of surface energy values, due to the heterogeneity among samples, even after averaging values from multiple measurements [72]. The contact angle is an excellent tool to generate qualitative information about successful surface treatment and different levels of surface coverage by comparing the affinity of the bio-based material (before and after treatment) with liquids of different polarities [62].

Figure 3. Contact angle measurement on a thin film of nanoparticles. On the left, a film obtained by compression of the particles, and on the right, a water drop on the surface of the film.

2.2.2. Inverse Gas Chromatography (IGC)

Inverse gas chromatography (IGC) is a versatile and robust adsorption method to characterize surface properties of a solid. Contrary to contact angle, IGC is independent of sample morphology, and solids in any form, including powders, fibers and with different crystalline and amorphous content can be evaluated. This is particularly suitable for surface characterization of small particles and porous materials with different chemistries, such as those of bio-based materials [66,73,74]. Moreover, IGC allows tight control of experimental conditions, including humidity and temperature that are not possible with other methods like contact angle, and which can significantly impact the measurement of surface activity. Hence, IGC provides more reliable quantitative information that can be used to predict the performance of filler reinforcement.

In IGC, solid particles and fibers are packed into a chromatography column as the stationary phase (Figure 4) [74,78]. The surface energy of fillers is determined by analyzing the retention time of probes, with known characteristics, which are injected as the mobile phase. These probes are injected at very low concentrations ("infinite dilution") to eliminate probe to probe interaction, so that interaction occurs only with the high-energy sites on the particle surface [74,78,79]. The probe retention times depend on the type and strength of the interaction between the filler material (stationary phase) and the specific probe [74,78,80], and are directly related to the thermodynamic interaction between the probes and the material surface [71,80,81].

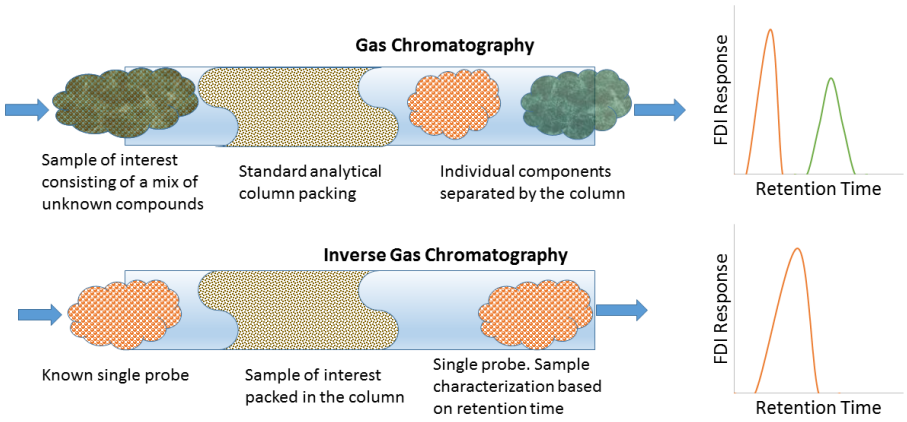

Figure 4. Comparison between gas chromatography and inverse gas chromatography columns. Adapted from References [74,82].

IGC has been extensively used for the characterization of complex and energetically heterogeneous materials like pharmaceutical carriers. Also, some studies have reported the use of IGC in bio-based materials, including mineral bone and eggshell particles and cellulosic materials [60,65,83]. These studies showed how IGC could effectively quantify differences in surface characteristics of materials, due to physicochemical changes caused by various grinding and drying conditions, and surface treatments. Moreover, the versatility of this method allows comparison with more conventional fillers like carbon black and silica [73,80] which can lead to a better understanding of differences in rubber reinforcement. Nevertheless, the main drawbacks of IGC are the need for more complicated setup and multiple, more expensive chemicals than other surface characterization techniques. Packing of the chromatographic columns can be time-consuming and introduce problems during measurements, such as pressure drops across the column, due to agglomeration of the particles.

2.3. Filler Chemistry

Chemistry-related variables can greatly impact the reinforcing effect of filler particles, directly or indirectly, but are often overlooked. Chemical composition of bio-based fillers defines their surface activity, chemical and thermal stability, and hence, composite performance [80]. The presence of

active chemical groups, like hydroxyl groups, on the filler surface, impedes interfacial adhesion of the filler to the rubber, resulting in poor reinforcement [40]. Chemical composition of agricultural and food processing residues is really diverse (Table 1) but, in general, they possess more polar surfaces than carbon black, due to their high surface concentration of active chemical groups. Although most research that has explored these residues as potential fillers for rubber has focused on the isolation of a single component, mainly calcium carbonate, cellulose, starch or chitin [8,84,85], the natural complex array of components in these residues could provide better reinforcement and improve other material properties. For instance, the presence of hydrophobic residual lignin and waxes in cellulose fibers may promote better adhesion than cellulose alone [42]. Moreover, high amounts of lignin can result in lower water absorption by the composite [31]. Unsaturated resins and proteins could behave as active ingredients in the vulcanization of the rubber or processing aids.

Table 1. Examples of agro-industrial residues studied as potential fillers for rubber and their main components.

Agricultural and Food Processing Residues	Main Composition	Reference
Banana fiber	Cellulose, hemicellulose, lignin	[8,46]
Carbon fly ash	Alumino-silicate, unburned carbon, iron oxide, calcium, potassium, magnesium, sodium, and sulfur compounds	[60,86,87]
Cassava bagasse	Starch and cellulose	[85,88]
Coir fiber	Lignin, cellulose and pectin	[6,89]
Eggshells	Calcium carbonate, proteins	[9,51]
Oil palm fiber	Cellulose, lignin and hemicellulose	[7,90]
Oil palm ash	Silicon dioxide, calcium oxide, potassium oxide, magnesium oxide and phosphorus pentoxide and unburned carbon	[91,92]
Rice husk	Cellulose, hemicellulose, lignin and Silicon dioxide	[93,94]
Rice husk ash	Silicon dioxide and unburned carbon	[14,95,96]
Shellfish	Chitin, calcium carbonate, protein	[13,84,97]
Soy hulls	Cellulose, hemicellulose, lignin, protein and pectin	[11,98,99]
Tomato peels	Cutin, pectin, cellulose and hemicellulose	[86,100,101]

Filler surface chemistry also affects the vulcanization behavior of filled compounds. Alkaline fillers can cure more quickly and lead to higher crosslink density unless the curing package is optimized to control the curing rate [10,40]. Active chemical groups on the surface of the filler can react with the compounding ingredients required to efficiently crosslink rubber molecules, reducing crosslink density and performance [40]. Likewise, active filler surfaces may absorb water, due to hydrogen bonding with water molecules [102]. In rubber composites, water adsorption may cause filler swelling compromising dimensional stability. Drying material to remove the adsorbed water may further weaken interfacial adhesion between the filler and the polymer and introduce flaws [38,89].

Nevertheless, chemically-active surfaces allow surface modification through grafting of molecules, or other physico-chemical treatments, to generate composites with unique properties [34,37,49,69]. For instance, grafting or coupling of fillers chemically attaches them to the rubber resulting in stronger polymer-filler interfaces and reduces filler-filler attraction which can lead to lower hysteresis in the material. Surface modifications often improve filler compatibility with the rubber, reduce reactivity with compounding ingredients, and inhibit moisture adsorption [40,89].

Chemical composition of the filler also defines its thermal stability, which is an important consideration in processing and aging of the composite. Low molecular weight components can degrade at rubber processing temperatures or operating conditions and adversely affect composite performance. Filler chemistry can be characterized by spectroscopic techniques, including Fourier transform infrared spectroscopy (FTIR), X-ray fluorescence spectroscopy (XRF), Energy-dispersive X-ray spectroscopy (EDX) and X-ray photoelectron spectroscopy (XPS) [38,73,93,103,104], to provide chemical group information and serve as a tool to evaluate the effectiveness of surface treatments.

A complete analysis of the material chemical composition can be performed using thermogravimetric analysis and chromatography.

2.3.1. Fourier Transform Infrared Spectroscopy

FTIR is the most commonly used filler surface characterization technique, due to its short characterization time, high signal-to-noise ratio, high accuracy in frequency, simplicity and because it can be used on almost any material [105]. Infrared spectroscopy uses the absorption of infrared radiation by a chemical bond in a molecule at a specific frequency (wave numbers) to provide information about functional groups and molecular structure. Absorption occurs when the bond vibrational frequency matches that of the infrared radiation. The vibration pattern is unique for a given molecule [106–108].

Peak intensity in a spectrum is proportional to the concentration of the corresponding bond or molecule. Therefore, IR spectroscopy can be used to quantify a particular component based on the Lambert–Beer law [106,107]:

$$A_v = \varepsilon_v bc, \tag{4}$$

where A_v is the absorbance at wave number v, ε_v is the molar absorption coefficient, b is the path length, and c is the concentration of the material. Nevertheless, due to structural complexities, it is unusual to find a single absorption frequency that can be used to quantify any single component. For instance, in bio-based materials, a large portion of organic components like lignin and cellulose can have overlapping bands with mineral materials. Hence, this technique is mostly used to obtain qualitative information. Quantitative analysis requires the use of standards, appropriate software and calibration with regression approaches [107]. Characterization of bio-based fillers with FTIR analysis identifies active chemical groups, or the lack thereof, resulting from surface treatment by comparisons with untreated materials. For example, analysis of hemp fibers treated with acetic and propionic anhydride resulted in absorbance increments in the regions 1737 and 1162–1229 cm^{-1} associated with stretching vibration of the carbonyl (C=O) group, and C–O stretching of the ester carboxyl group, due to the esterification of the fibers [38]. However, FTIR does not provide quantitative information on the extent of surface treatment-induced changes.

Although FTIR can be performed in transmission or reflection mode, recently, the attenuated total reflection (ATR) mode has become the most commonly used method for the surface characterization of fillers [38,69,107,109]. ATR-FTIR is done by bringing the filler into direct contact with a crystalline material containing prisms that act as an internal reflection element. Although this is an easy and fast way to characterize a material surface, it does not account for changes in functional groups caused by heat during processing of the composite.

Another important parameter to consider when using ATR-FTIR or any surface characterization technique is the depth of penetration. In ATR-FTIR, the depth of infrared radiation penetration depends on wavelength, incident angle, and indices of prism and sample refraction [108,110]:

$$d_p = \frac{1}{2\Pi v\left(sin^2\,\theta - \left(\frac{n_2}{n_1}\right)^2\right)^{\frac{1}{2}}}, \tag{5}$$

where d_p is the penetration depth, v is the infrared radiation frequency, n_2 and n_1 are the refraction indexes of the sample and the prism, respectively, and θ is the incident angle.

Crystalline materials used as prisms include diamond (C), germanium (Ge), silicon (Si), zinc selenide (ZnSe) and thallium bromide (KRS-5) [107,108]. These materials have different indices of refraction (Table 2), as well as different robustness and cost. Prism selection depends on the type of material to be characterized. For instance, samples that strongly absorb infrared radiation, like carbon black, need a lower depth of penetration to avoid overabsorption. In general, the lower the prism refractive index, the higher the penetration depth [108]. In addition, if the samples to be characterized are abrasive, a more robust prism may be desired.

Table 2. Characteristics of crystalline materials used as prism for attenuated total reflection-Fourier transform infrared (ATR-FTIR) [108].

Material	Index of Refraction	Hardness (Kg/mm^2)
Diamond	2.40	5700
Germanium	4.00	550
Silicon	3.42	1150
Zinc selenide	2.42	120
Thallium bromide	2.35	40

2.3.2. X-ray Spectroscopy

Different X-ray spectroscopy techniques, including XPS, XRF and EDX, can be used to evaluate the elemental composition of fillers. X-ray spectroscopic methods are non-destructive techniques based on the principle that each element has a unique response to a high-energy beam. These techniques are particularly useful for the chemical characterization of bio-based fillers with high mineral content, such as rice husk or mollusk shells [111,112], but can also be used in other compositionally diverse materials to identify trace elements, state of oxidation and variations in carbon/oxygen ratio as result of filler extraction method, purification or surface treatments. For instance, XPS can quantify differences in O/C ratio in cellulosic fibers from different sources and variation of the O/C ratio as a result of acetylation [38].

Interfacial interaction between non-polar rubbers and more polar bio-based fillers is a well-known variable affecting reinforcement of rubber composites. However, the performance of the rubber has not been correlated quantitatively to the polarity of different bio-based fillers. X-ray spectroscopy is an important tool to further understand and quantify these differences. Although all these techniques are very sensitive and provide qualitative and quantitative information about the elemental composition of a material surface, and information about associated functional groups, each technique has its own limitations in terms of the spatial resolution (electron penetration depth) and the information they provide [110,113]. Statistical analysis has been used to classify different carbon blacks based on surface chemistry information obtained from XPS and thermal analysis-mass spectroscopy (TGA-MS) and IGC [73].

X-ray spectroscopy techniques require very sophisticated instrumentation. Moreover, data interpretation becomes more difficult as the complexity of the material increases, bio-based materials often are multiphasic and possess complex composition. Furthermore, the reliability of the results is highly dependent on sample preparation.

2.3.3. Thermogravimetric Analysis (TGA)

Thermal analysis is a crucial test for bio-based fillers, due to the high temperature required for vulcanization and during the life of finished rubber composites. Thermal decomposition of the filler can negatively affect the performance of the material by creating voids in the material or simply not achieving the expected reinforcement. Although TGA is mainly used to determine the thermal stability of the filler, it can also provide information about the chemical composition of the material, by separating different constituent fractions within the material, for instance, moisture, organic and inorganic fraction.

TGA measures the mass loss upon heating, and each step of mass loss marks changes in the sample, due to decomposition and chemical reactions [114], and such changes can be used to evaluate polymer filler interactions and surface modifications. For example, TGA has been used to correlate weight loss in a specific temperature range to the amount of condensation water lost from silanol groups which, in turn, was used to estimate silanol group density [61]. In this study, rice hull ash had a lower silanol density than commercial silica, which reduced the efficiency of surface treatments intended to improve its interaction with rubber.

In bio-based fillers, small organic molecules and impurities can quantitatively affect both processing and performance of composites. For instance, resin in lignocellulosic materials has been associated with low composite modulus [9]. TGA can be coupled to additional gas analysis techniques, such as FTIR, gas chromatography with mass spectroscopy (GC-MS) to provide both quantitative and qualitative information about the decomposition and chemical make-up of the filler [114–116]. TGA coupled with MS was used to detect and quantify the presence of sulfate groups in cellulose nanocrystals. Moreover, the grafting of molecules on the surface of the filler and changes in crystallinity can also be determined by thermal analysis [117]. Nevertheless, despite the multiple advantages of using TGA alone or coupled with other analytical tools, exact chemical characterization in some materials can be challenging. In TG/FTIR or TG/MS, identification of specific components is complicated when gases generated in TGA have overlapping spectra. Also, although TG/GC-MS allows the composition of the evolved gases from the organic fraction of a material to be separated and identified, is not possible to assign a specific mass loss to each component because of the retention in the chromatographic column [118]. Elemental analysis of the ash must be performed to characterize the inorganic fraction.

2.4. Shape and Structure

Conventional fillers have well-defined shapes, including spheres (carbon black and silica), and plates (mica, talc and kaolin). While fillers obtained from bio-based sources may have a wider variety of shapes, including elongated rod-like shaped (cellulosic fibers or crystals) and undefined irregular shapes (particles that resulted from grinding) (Figure 5) [40,44]. Nevertheless, similar to conventional fillers, small primary particles can aggregate into complex tri-dimensional objects, due to bonding forces between the filler particles [19]. The random spatial arrangement of primary particles generates different degrees of irregularity that define the effective filler structure [18]. Moreover, for bio-based filler complex structure also can result from naturally occurring pores, intermeshed fibers and surface roughness.

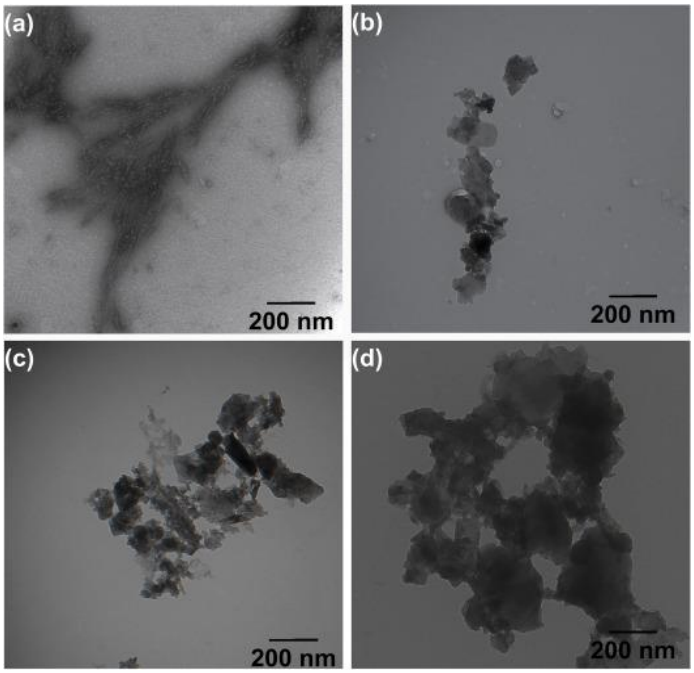

Figure 5. Examples of various filler particle shapes: (**a**) Cellulose nanocrystals from guayule bagasse; nanosized particles obtained from (**b**) carbon fly ash, (**c**) eggshells, and (**d**) tomato peels. Reproduced with permission from reference [55].

Filler structure contributes to composite reinforcement by mechanically interlocking the polymer chains, which restricts their mobility when subject to deformation [18,41]. Branching of filler aggregates

defines the effective filler volume fraction in the polymer and, therefore, contributes to the hydrodynamic effect of the filler in the polymer [16].

Particle shape and structure are easy to describe qualitatively, but are difficult to measure quantitatively. This is particularly true for fillers obtained from agricultural and food processing residues in which shape and structure are diverse and can vary depending on the source and method used to prepare the particles [49,119]. Furthermore, different structures may coexist in the same filler, due to random aggregation and source heterogeneity [16,49].

Structure of conventional fillers, like carbon black, can be characterized as the volume of dibutylphthalate (DBP) absorbed [16,18]. However, this measurement only represents the empty volume between particles and agglomerates and does not describe the primary particle shape or structure. Furthermore, DBP absorption is sensitive to the filler surface chemistry, so it an unreliable measurement for most non-black fillers [16]. Other methods include microscopy techniques like scanning electron microscopy (SEM), transmission electron microscopy (TEM), and atomic force microscopy (AFM).

2.4.1. Electron Microscopy

Electron microscopy techniques are widely used to characterize filler shape and structure, due to their high spatial resolution [120]. However, these techniques provide mainly qualitative information, are very time-consuming, results are highly dependent on sample selection and preparation, and only a few particles/aggregates can be observed at one time [16,41], which is a problem when 200 measurements may be needed [117]. Despite the lack of quantitative data, electron microscopy is heavily relied upon to assess filler dispersion and polymer-filler interactions [120,121].

Scanning electron microscopy (SEM) uses an electron beam to scan a material surface and visualize morphological features which can be filler dependent. Electron interaction with a surface generates specific electron signals that are detected and converted into magnified two-dimensional images [87,120,122]. SEM resolution is limited to approximately 10 nm, and so SEM is generally used to characterize particles at the micron scale [120]. SEM also is used to characterize fracture surfaces of rubber composites, analyze filler dispersion, and the presence of voids and aggregates [120,121]. SEM requires conductive surfaces; hence, fillers and rubber composites must be sputter coated with a layer of conductive material before analysis [120,123].

Like SEM, transmission electron microscopy (TEM) uses an electron source, electron lenses and electron detectors. However, in TEM, the electrons pass through the sample [110,122], and have higher electron energies and smaller focal lengths and, hence, higher resolution than SEM. Sections must be less than 100 nm thick, to allow free passage of electrons through the sample with relatively little loss of energy [120,122]. Staining is generally used to improve contrast and highlight different components in particles obtained from agricultural and food processing residues.

TEM is preferred for nanosized filler characterization [122]. TEM allows characterization of the shape of individual nanoparticles, particle dispersion within the composite, and the filler network. Multiple imaging of a sample at various angles can produce a three-dimensional representation of the sample [120,124].

2.4.2. Atomic Force Microscopy (AFM)

AFM is mainly used to analyze topographical features of composite surfaces, but has been used to evaluate the structure, shape and the elastic modulus of single particles [11,42,54,120,125]. This technique uses a sharp tip (radius of 10–100 nm), supported in a cantilever, to scan the surface of a sample. A laser beam is focused on the cantilever and monitors and records its deformation as a result of topographical variation in the sample surface [110,120]. AFM has a higher resolution than SEM and can be used to evaluate nanosized particles. However, similar to SEM, this analysis is limited to surfaces.

AFM offers three-dimensional surface images and does not require sample sputter coating [124]. Nevertheless, limitations of AFM include its lower canning speed compared to SEM and tip artefacts like tip/sample broadening, which may overestimate the size of particles obtained agricultural and food processing residue [11,126].

2.5. Filler Crystallinity

Crystallinity is not a characteristic evaluated in conventional fillers, but can have both direct and indirect effect on rubber reinforcement and so it is important to evaluate for mineral and lignocellulosic fillers. Filler crystallinity can affect the filler surface activity, and hence, its interaction with rubber. Amorphous regions can concentrate on structural defects that translate into high energy sites [19,67]. Plant fibers and calcium carbonate particles have consistently displayed lower dispersive components of surface energy typical of materials with lower crystallinity [66,67]. Crystallinity impacts particle tensile strength, modulus and water resistance, and so affects their reinforcing potential [11,31,54,127]. Furthermore, crystalline materials have a lower tendency to undergo physical and chemical changes than amorphous materials [128], creating better composite stability. Changes in crystallinity also can indicate compound purity, such as in the purification of cellulose nanocrystals.

X-ray diffraction (XRD) is the most commonly used technique to quantify the amount of crystallinity [49,119,128,129]. The percentage of crystallinity is obtained from the ratio of crystalline peak area to the total XRD intensity profiles [130,131]:

$$crystallinity = \frac{A_c}{A_c + A_a} \times 100, \quad (6)$$

where A_c is the crystalline area, and A_a is the amorphous area on the X-ray diffractogram.

Calculation of crystallinity depends on the decomposition of the total XRD intensity profiles into the amorphous and the crystalline components. This separation of components can be challenging and represents the main limitation of XRD characterization of bio-based fillers [128].

Different quantification methods have been used to quantify the crystalline and amorphous components of total XRD intensity profiles. One method evaluates total XRD profile decomposition by curve fitting using Gaussian, Lorentzian, and Voigt functions to separate the crystalline and amorphous components [123,132,133]. Another method uses the Ruland–Vonk or amorphous contribution subtraction method in which the profile obtained from a standard material is subtracted from the total XRD profile [123,133]. The Segel or peak height method is particularly used for lignocellulosic materials. In this method, crystallinity is calculated from the equation [123,133,134]:

$$Crystallinity = \frac{(I_{200} - I_{\mathrm{am}})}{I_{200}} \times 100, \quad (7)$$

where I_{200} is the maximum peak intensity at $2\theta = 22.6°$, and I_{am} is the minimum peak intensity between the (2 0 0) and (1 1 0) peaks at $2\theta = 18°$ [123,135]. These different methods may produce considerably different results [132].

Characteristic diffraction peaks also can help identify differences in crystal structure between conventional mineral fillers and fillers obtained from agricultural and food processing residues. The crystal phase of calcium carbonate obtained from seashells is mostly aragonite and calcite, whilst the vaterite crystal phase is only seen in synthetic materials [111].

3. Conclusions

Agricultural and food processing residues offer a wide variety of materials to explore as potential sustainable fillers for rubber composites. As these alternative filler sources are considered, we need to better understand and quantify filler characteristics which affect their reinforcement efficiency in rubber composites. Given the diversity among these materials, comprehensive selection criteria

beyond particle size and surface polarity must be developed. Therefore, appropriate characterization techniques are needed to fully understand these materials, and potential performance and cost advantages over traditional fillers. Although some characterization methods applied to conventional fillers can be used for alternative fillers, new and modified methods are required, due to the inherent differences in chemistry and morphology of these residue-derived materials. Furthermore, the efficacy of such fillers should always be compared to the conventional fillers, and filler combinations hold considerable promise.

Author Contributions: Conceptualization, C.S.B. and K.C.; formal analysis, C.S.B. and K.C.; investigation, C.S.B. and K.C.; writing—original draft preparation, C.S.B.; writing—review and editing, K.C.

Funding: This research received no external funding.

Conflicts of Interest: The authors declare no conflict of interest.

References

1. Mirabella, N.; Castellani, V.; Sala, S. Current options for the valorization of food manufacturing waste: A review. *J. Clean. Prod.* **2014**, *65*, 28–41. [CrossRef]
2. Pfaltzgraff, L.A.; Cooper, E.C.; Budarin, V.; Clark, J.H. Food waste biomass: A resource for high-value chemicals. *Green Chem.* **2013**, *15*, 307–314. [CrossRef]
3. Deniel, M.; Haarlemmer, G.; Roubaud, A.; Weiss-Hortala, E.; Fages, J. Energy valorisation of food processing residues and model compounds by hydrothermal liquefaction. *Renew. Sustain. Energy Rev.* **2016**, *54*, 1632–1652. [CrossRef]
4. FAO. The Food Systems of the Future Need to be Smarter, More Efficiente, (n.d.). Available online: http://www.fao.org/news/story/en/item/275009/icode/ (accessed on 19 September 2019).
5. ASTM International. *Standard Terminology for Composite Materials*; ASTM International: West Conshohocken, PA, USA, 2016. [CrossRef]
6. Geethamma, V.G.; Kalaprasad, G.; Groeninckx, G.; Thomas, S. Dynamic mechanical behavior of short coir fiber reinforced natural rubber composites. *Compos. Part A Appl. Sci. Manuf.* **2005**, *36*, 1499–1506. [CrossRef]
7. Jacob, M.; Thomas, S.; Varughese, K.T. Mechanical properties of sisal/oil palm hybrid fiber reinforced natural rubber composites. *Compos. Sci. Technol.* **2004**, *64*, 955–965. [CrossRef]
8. Abraham, E.; Deepa, B.; Pothan, L.A.; John, M.; Narine, S.S.; Thomas, S. Physicomechanical properties of nanocomposites based on cellulose nanofibre and natural rubber latex. *Cellulose* **2013**, *20*, 417–427. [CrossRef]
9. Barrera, C.S.; Cornish, K. Novel mineral and organic materials from agro-industrial residues as fillers for natural rubber. *J. Polym. Environ.* **2015**, *23*, 437–448. [CrossRef]
10. Barrera, C.S.; Cornish, K. High performance waste-derived filler/carbon black reinforced guayule natural rubber composites. *Ind. Crops Prod.* **2016**, *86*, 132–142. [CrossRef]
11. Neto, W.P.F.; Mariano, M.; Da Silva, I.S.V.; Silvério, H.A.; Putaux, J.L.; Otaguro, H. Mechanical properties of natural rubber nanocomposites reinforced with high aspect ratio cellulose nanocrystals isolated from soy hulls. *Carbohydr. Polym.* **2016**, *153*, 143–152. [CrossRef]
12. Intharapat, P.; Kongnoo, A.; Kateungngan, K. The Potential of Chicken Eggshell Waste as a Bio-filler Filled Epoxidized Natural Rubber (ENR) Composite and its Properties. *J. Polym. Environ.* **2013**, *21*, 245–258. [CrossRef]
13. Poompradub, S.; Ikeda, Y.; Kokubo, Y.; Shiono, T. Cuttlebone as reinforcing filler for natural rubber. *Eur. Polym. J.* **2008**, *44*, 4157–4164. [CrossRef]
14. Sae-Oui, P.; Rakdee, C.; Thanmathorn, P. Use of rice husk ash as filler in natural rubber vulcanizates: In comparison with other commercial fillers. *J. Appl. Polym. Sci.* **2002**, *83*, 2485–2493. [CrossRef]
15. Samsuri, A.B. Theory and Mechanisms of Filler Reinforcement in Natural Rubber. In *Natural Rubber Materials: Volume 2: Composites and Nanocomposites*; Thomas, H.M.S., Chan, C.H., Pothen, L., Joy, J., Eds.; The Royal Society of Chemistry: London, UK, 2013; pp. 73–111. [CrossRef]
16. Donnet, J.B.; Custodero, E. Reinforcement of Elastomers by Particulate Fillers. In *The Science and Technology of Rubber*, 4th ed.; Mark, J.E., Erman, B., Roland, M., Eds.; Elsevier: Amsterdam, The Netherlands, 2013; pp. 383–416. [CrossRef]

17. Rattanasom, N.; Saowapark, T.A.; Deeprasertkul, C. Reinforcement of natural rubber with silica/carbon black hybrid filler. *Polym. Test.* **2007**, *26*, 369–377. [CrossRef]
18. Fröhlich, J.; Niedermeier, W.; Luginsland, H.D. The effect of filler-filler and filler-elastomer interaction on rubber reinforcement. *Compos. Part A Appl. Sci. Manuf.* **2005**, *36*, 449–460. [CrossRef]
19. Leblanc, J. Rubber–filler interactions and rheological properties in filled compounds. *Prog. Polym. Sci.* **2002**, *27*, 627–687. [CrossRef]
20. Hamed, G.R. Reinforcement of Rubber. *Rubber Chem. Technol.* **2000**, *73*, 524–533. [CrossRef]
21. Rader, C.P. Vulcanization of rubber-Sulfur and non-peroxides. In *Basic Elastomer Technol*; Baranwal, K.C., Stephens, H.L., Eds.; American Chemical Society, Rubber Division: Akron, OH, USA, 2001; pp. 165–190.
22. Coran, A.Y. Vulcanization. In *The Science and Technology of Rubber*, 2nd ed.; Elsevier: Amsterdam, The Netherlands, 2013; pp. 337–381. [CrossRef]
23. Notch Consulting Inc. Carbon black and silica in the tire markets challenges and opportunities. In Proceedings of the Tire Technology Expo, Cologne, Germany, 7 February 2015.
24. Malaysian Rubber Board. Natural Rubber Statistics. 2016. Available online: http://www.lgm.gov.my/nrstat/nrstats.pdf (accessed on 24 October 2019).
25. International Carbon Black Association. Carbon Black User's Guide. 2004. Available online: http://www.carbon-black.org/files/carbonblackuserguide.pdf (accessed on 18 September 2019).
26. Studebaker, M. The chemistry of carbon black and reinforcement. *Rubber Chem. Technol.* **1957**, *30*, 1401–1483. [CrossRef]
27. Gerspacher, M.; Wampler, W. Fillers—Carbon black. In *Basic Elastomer Technol*; Baranwal, K.C., Stephens, H., Eds.; American Chemical Society, Rubber Division: Akron, OH, USA, 2001; pp. 57–81.
28. Barrera, C.S.; Cornish, K. Waste-derived Reinforcing Fillers in Guayule and Hevea Natural Rubber. In Proceedings of the 190th Technical Meeting Rubber Division American Chemical Society, Pittsburg, PA, USA, 10 October 2016.
29. Moore, M. Exec: Expect Carbon Black Shortage in Five Years. 2015. Available online: http://www.rubbernews.com/article/20150717/NEWS/307139999 (accessed on 16 Auguest 2016).
30. Afiq, M.M.; Azura, A.R. Effect of sago starch loadings on soil decomposition of Natural Rubber Latex (NRL) composite films mechanical properties. *Int. Biodeterior. Biodegrad.* **2013**, *85*, 139–149. [CrossRef]
31. Nunes, R.C.R. *Natural Rubber (NR) Composites Using Cellulosic Fiber Reinforcements in Chemistry, Manufacture and Applications of Natural Rubber*; Elsevier: Amsterdam, The Netherlands, 2014; pp. 284–302. [CrossRef]
32. John, M.J.; Thomas, S. Biofibres and biocomposites. *Carbohydr. Polym.* **2008**, *71*, 343–364. [CrossRef]
33. Angellier, H.; Molina-Boisseau, S.; Dufresne, A. Mechanical properties of waxy maize starch nanocrystal reinforced natural rubber. *Macromolecules* **2005**, *38*, 9161–9170. [CrossRef]
34. Parambath Kanoth, B.; Claudino, M.; Johansson, M.; Berglund, L.A.; Zhou, Q. Biocomposites from natural rubber: Synergistic effects of functionalized cellulose nanocrystals as both reinforcing and crosslinking agents via free-radical thiol–ene chemistry. *ACS Appl. Mater. Interfaces.* **2015**, *7*, 16303–16310. [CrossRef] [PubMed]
35. Liu, C.; Shao, Y.; Jia, D. Chemically modified starch reinforced natural rubber composites. *Polymer* **2008**, *49*, 2176–2181. [CrossRef]
36. Laurichesse, S.; Avérous, L. Chemical modification of lignins: Towards biobased polymers. *Prog. Polym. Sci.* **2014**, *39*, 1266–1290. [CrossRef]
37. Mihajlović, S.R.; Vučinić, D.R.; Sekulić, Ž.T.; Milićević, S.Z.; Kolonja, B.M. Mechanism of stearic acid adsorption to calcite. *Powder Technol.* **2013**, *245*, 208–216. [CrossRef]
38. Tserki, V.; Zafeiropoulos, N.E.; Simon, F.; Panayiotou, C. A study of the effect of acetylation and propionylation surface treatments on natural fibres. *Compos. Part A Appl. Sci. Manuf.* **2005**, *36*, 1110–1118. [CrossRef]
39. Chenal, J.M.; Gauthier, C.; Chazeau, L.; Guy, L.; Bomal, Y. Parameters governing strain induced crystallization in filled natural rubber. *Polymer* **2007**, *48*, 6893–6901. [CrossRef]
40. Byers, J.T. Filler—Non-black. In *Basic Elastomer Technol*; Baranwal, K.C., Stephens, H.L., Eds.; American Chemical Society, Rubber Division: Akron, OH, USA, 2001; pp. 82–111.
41. Kohls, D.J.; Beaucage, G. Rational design of reinforced rubber. *Curr. Opin. Solid State Mater. Sci.* **2002**, *6*, 183–194. [CrossRef]
42. Bendahou, A.; Kaddami, H.; Dufresne, A. Investigation on the effect of cellulosic nanoparticles' morphology on the properties of natural rubber based nanocomposites. *Eur. Polym. J.* **2010**, *46*, 609–620. [CrossRef]

43. Khan, I.; Bhat, A. Micro and Nano Calcium Carbonate Filled Natural Rubber Composites and Nanocomposites. In *Natural Rubber Materials*; Thomas, H.M.S., Chan, C.H., Pothen, L., Joy, J., Eds.; The Royal Society of Chemistry: London, UK, 2014; pp. 467–487. [CrossRef]
44. Szeluga, U.; Kumanek, B.; Trzebicka, B. Synergy in hybrid polymer/nanocarbon composites. A review. *Compos. Part A Appl. Sci. Manuf.* **2015**, *73*, 204–231. [CrossRef]
45. Peddini, S.K.; Bosnyak, C.P.; Henderson, N.M.; Ellison, C.J.; Paul, D.R. Nanocomposites from styrene-butadiene rubber (SBR) and multiwall carbon nanotubes (MWCNT) part 1: Morphology and rheology. *Polymer* **2014**, *55*, 258–270. [CrossRef]
46. Abraham, E.; Deepa, B.; Pothan, L.A.; Jacob, M.; Thomas, S.; Cvelbar, U. Extraction of nanocellulose fibrils from lignocellulosic fibres: A novel approach. *Carbohydr. Polym.* **2011**, *86*, 1468–1475. [CrossRef]
47. Fang, Q.; Song, B.; Tee, T.T.; Sin, L.T.; Hui, D.; Bee, S.T. Investigation of dynamic characteristics of nano-size calcium carbonate added in natural rubber vulcanizate. *Compos. Part B Eng.* **2014**, *60*, 561–567. [CrossRef]
48. Galimberti, M.; Cipolletti, V.; Kumar, V. Nanofillers in Natural Rubber. In *Natural Rubber Materials Volume 2 Composites Nanocomposites*; Thomas, S., Chan, C.H., Pothen, L., Joy, J., Maria, H., Eds.; The Royal Society of Chemistry: London, UK, 2014; pp. 34–72. [CrossRef]
49. Bandyopadhyay-Ghosh, S.; Ghosh, S.B.; Sain, M. The use of biobased nanofibres in composites. In *Biofiber Reinforcements in Composite Materials*; Faruk, O., Sain, M., Eds.; Elsevier: Amsterdam, The Netherlands, 2015; pp. 571–647. [CrossRef]
50. Paul, K.T.; Satpathy, S.K.; Manna, I.; Chakraborty, K.K.; Nando, G.B. Preparation and characterization of nano structured materials from fly ash: A waste from thermal power stations, by high energy ball milling. *Nanoscale Res. Lett.* **2007**, *2*, 397–404. [CrossRef]
51. Hassan, T.A.; Rangari, V.K.; Rana, R.K.; Jeelani, S. Sonochemical effect on size reduction of $CaCO_3$ nanoparticles derived from waste eggshells. *Ultrason. Sonochem.* **2013**, *20*, 1308–1315. [CrossRef] [PubMed]
52. Chao, H.; Riggleman, R.A. Effect of particle size and grafting density on the mechanical properties of polymer nanocomposites. *Polymer* **2013**, *54*, 5222–5229. [CrossRef]
53. Kueseng, K.; Jacob, K.I. Natural rubber nanocomposites with SiC nanoparticles and carbon nanotubes. *Eur. Polym. J.* **2006**, *42*, 220–227. [CrossRef]
54. Siqueira, G.; Bras, J.; Dufresne, A. Cellulosic bionanocomposites: A review of preparation, properties and applications. *Polymers* **2010**, *2*, 728–765. [CrossRef]
55. Barrera, C.S.; Cornish, K. Processing and mechanical properties of natural rubber/waste-derived nano fi ller composites compared to macro and micro filler composites. *Ind. Crop. Prod.* **2017**, *107*, 217–231. [CrossRef]
56. Fagerlund, G. Determination of specific surface by the BET method. *Matériaux Constr.* **1973**, *6*, 239–245. [CrossRef]
57. Brunauer, S.; Emmett, P.H.; Teller, E. Adsorption of Gases in Multimolecular Layers. *J. Am. Chem. Soc.* **1938**, *60*, 309–319. [CrossRef]
58. ASTM International. *Standard Test Method for Carbon Black—Total and External Surface Area by Nitrogen*; ASTM International: West Conshohocken, PA, USA, 2016. [CrossRef]
59. Thommes, M.; Kaneko, K.; Neimark, A.V.; Olivier, J.P.; Rodriguez-Reinoso, F.; Rouquerol, J. Physisorption of gases, with special reference to the evaluation of surface area and pore size distribution (IUPAC Technical Report). *Pure Appl. Chem.* **2015**, *87*, 1051–1069. [CrossRef]
60. Barrera, C.S.; Soboyejo, A.B.O.; Cornish, K. Quantification of the contribution of filler characteristics to natural rubber reinforcement using principal componentanalysis. *Rubber Chem. Technol.* **2018**, *91*, 79–96. [CrossRef]
61. Chaudhary, D.S.; Jollands, M.C. Characterization of rice hull ash. *J. Appl. Polym. Sci.* **2004**, *93*, 1–8. [CrossRef]
62. Papirer, E.; Schultz, J.; Turchi, C. Surface properties of a calcium carbonate filler treated with stearic acid. *Eur. Polym. J.* **1984**, *20*, 1155–1158. [CrossRef]
63. Stöckelhuber, K.W.; Svistkov, A.S.; Pelevin, A.G.; Heinrich, G. Impact of filler surface modification on large scale mechanics of styrene butadiene/silica rubber composites. *Macromolecules* **2011**, *44*, 4366–4381. [CrossRef]
64. Papirer, E.; Balard, H.; Vidal, A. Inverse gas chromatography: A valuable method for the surface characterization of fillers for polymers (glass fibres and silicas). *Eur. Polym. J.* **1988**, *24*, 783–790. [CrossRef]
65. Hole, B.B.; Keller, D.S.; Burry, W.M.; Schwarz, J.A. Surface energetics of bone mineral and synthetic hydroxyapatite using inverse gas chromatography. *J. Chromatogr. B* **2011**, *879*, 1847–1850. [CrossRef]

66. Cordeiro, N.; Gouveia, C.; Moraes, A.G.O.; Amico, S.C. Natural fibers characterization by inverse gas chromatography. *Carbohydr. Polym.* **2011**, *84*, 110–117. [CrossRef]
67. Burry, W.M.; Keller, D.S. Effects of dehydration on the apolar surface energetics of inorganic paper fillers. *J. Chromatogr. A* **2002**, *972*, 241–251. [CrossRef]
68. Papirer, E.; Brendle, E.; Ozil, F.; Balard, H. Comparison of the surface properties of graphite, carbon black and fullerene samples, measured by inverse gas chromatography. *Carbon* **1999**, *37*, 1265–1274. [CrossRef]
69. Cordeiro, N.; Gouveia, C.; John, M.J. Investigation of surface properties of physico-chemically modified natural fibres using inverse gas chromatography. *Ind. Crops Prod.* **2011**, *33*, 108–115. [CrossRef]
70. Nardin, M.; Balard, H.; Papirer, E. Surface characteristics of commercial carbon fibres determined by inverse gas chromatography. *Carbon* **1990**, *28*, 43–48. [CrossRef]
71. Voelkel, A.; Strzemiecka, B.; Adamska, K.; Milczewska, K. Inverse gas chromatography as a source of physiochemical data. *J. Chromatogr. A* **2009**, *1216*, 1551–1566. [CrossRef] [PubMed]
72. Stöckelhuber, K.W.; Das, A.; Jurk, R.; Heinrich, G. Contribution of physico-chemical properties of interfaces on dispersibility, adhesion and flocculation of filler particles in rubber. *Polymer* **2010**, *51*, 1954–1963. [CrossRef]
73. Strzemiecka, B.; Voelkel, A.; Donate-Robles, J.; Martín-Martínez, J.M. Assessment of the surface chemistry of carbon blacks by TGA-MS, XPS and inverse gas chromatography using statistical chemometric analysis. *Appl. Surf. Sci.* **2014**, *316*, 315–323. [CrossRef]
74. Mohammadi-Jam, S.; Waters, K.E. Inverse gas chromatography applications: A review. *Adv. Colloid Interface Sci.* **2014**, *212*, 21–44. [CrossRef]
75. Gamble, J.F.; Leane, M.; Olusanmi, D.; Tobyn, M.; Šupuk, E.; Khoo, J. Surface energy analysis as a tool to probe the surface energy characteristics of micronized materials—A comparison with inverse gas chromatography. *Int. J. Pharm.* **2012**, *422*, 238–244. [CrossRef]
76. Riedl, B.; Matuana, L.M. Inverse Gas Chromatography of Fibers and Polymers, (2006). In *Encyclopedia of Surface and Colloid Science*; CRC Press: Boca Raton, FL, USA, 2015; pp. 3352–3364. [CrossRef]
77. Grimsey, I.M.; Feeley, J.C.; York, P. Analysis of the surface energy of pharmaceutical powders by inverse gas chromatography. *J. Pharm. Sci.* **2002**, *91*, 571–583. [CrossRef]
78. Thielmann, F. Introduction into the characterisation of porous materials by inverse gas chromatography. *J. Chromatogr. A* **2004**, *1037*, 115–123. [CrossRef]
79. Charmas, B.; Leboda, R. Effect of surface heterogeneity on adsorption on solid surfaces: Application of inverse gas chromatography in the studies of energetic heterogeneity of adsorbents. *J. Chromatogr. A* **2000**, *886*, 133–152. [CrossRef]
80. Rückriem, M.; Inayat, A.; Enke, D.; Gläser, R.; Einicke, W.-D.; Rockmann, R. Inverse gas chromatography for determining the dispersive surface energy of porous silica. *Colloids Surf. A Physicochem. Eng. Asp.* **2010**, *357*, 21–26. [CrossRef]
81. Van Asten, A.; van Veenendaal, N.; Koster, S. Surface characterization of industrial fibers with inverse gas chromatography. *J. Chromatogr. A* **2000**, *888*, 175–196. [CrossRef]
82. Thielmann, F.; Levoguer, C. *Inverse Gas Chromatography i GC—A New Instrumental Technique for Characterising the Phyisco-Chemical Properties of Pharmaceutical Materials*; Surface Measurement Systems Ltd.: London, UK, 2001; pp. 1–9.
83. Cordeiro, N.; Ornelas, M.; Ashori, A.; Sheshmani, S.; Norouzi, H. Investigation on the surface properties of chemically modified natural fibers using inverse gas chromatography. *Carbohydr. Polym.* **2012**, *87*, 2367–2375. [CrossRef]
84. Nair, K.G.; Dufresne, A. Crab shell chitin whisker reinforced natural rubber nanocomposites. 1. Processing and swelling behavior. *Biomacromolecules* **2003**, *4*, 657–665. [CrossRef]
85. Pasquini, D.; Teixeira, E.D.M.; Curvelo, A.A.D.S.; Belgacem, M.N.; Dufresne, A. Extraction of cellulose whiskers from cassava bagasse and their applications as reinforcing agent in natural rubber. *Ind. Crops Prod.* **2010**, *32*, 486–490. [CrossRef]
86. Kutchko, B.G.; Kim, A.G. Fly ash characterization by SEM-EDS. *Fuel* **2006**, *85*, 2537–2544. [CrossRef]
87. Sombatsompop, N.; Thongsang, S.; Markpin, T.; Wimolmala, E. Fly ash particles and precipitated silica as fillers in rubbers. I. Untreated fillers in natural rubber and styrene-butadiene rubber compounds. *J. Appl. Polym. Sci.* **2004**, *93*, 2119–2130. [CrossRef]
88. Pandey, A.; Soccol, C.R.; Nigam, P.; Soccol, V.T.; Vandenberghe, L.P.S.; Mohan, R. Biotechnological potential of agro-industrial residues. II: Cassava bagasse. *Bioresour. Technol.* **2000**, *74*, 81–87. [CrossRef]

89. Geethamma, V.G.; Thomas, S. Diffusion of water and artificial seawater through coir fiber reinforced natural rubber composites. *Polym. Compos.* **2005**, *26*, 136–143. [CrossRef]
90. Shinoj, S.; Visvanathan, R.; Panigrahi, S.; Kochubabu, M. Oil palm fiber (OPF) and its composites: A review. *Ind. Crops Prod.* **2011**, *33*, 7–22. [CrossRef]
91. Ismail, H.; Haw, F.S. Effects of palm ash loading and maleated natural rubber as a coupling agent on the properties of palm-ash-filled natural rubber composites. *J. Appl. Polym. Sci.* **2008**, *110*, 2867–2876. [CrossRef]
92. Ooi, Z.X.; Ismail, H.; Bakar, A.A. Synergistic effect of oil palm ash filled natural rubber compound at low filler loading. *Polym. Test.* **2013**, *32*, 38–44. [CrossRef]
93. Johar, N.; Ahmad, I.; Dufresne, A. Extraction, preparation and characterization of cellulose fibres and nanocrystals from rice husk. *Ind. Crops Prod.* **2012**, *37*, 93–99. [CrossRef]
94. Khalf, A.I.; Ward, A.A. Use of rice husks as potential filler in styrene butadiene rubber/linear low density polyethylene blends in the presence of maleic anhydride. *Mater. Des.* **2010**, *31*, 2414–2421. [CrossRef]
95. Ismail, H.; Nizam, J.M.; Khalil, H.P.S.A. Effect of a compatibilizer on the mechanical properties and mass swell of white rice husk ash filled natural rubber/linear low density polyethylene blends. *Polym. Test.* **2001**, *20*, 125–133. [CrossRef]
96. Rashid, A.A.; Yahya, S.R. Mechanical Properties of Natural Rubber Composites Filled with Macro and Nanofillers. In *Natural Rubber Materials*; Thomas, S., Chan, C.H., Pothen, L., Joy, J., Maria, H., Eds.; The Royal Society of Chemistry: London, UK, 2013; Volume 2, pp. 550–573. [CrossRef]
97. Poompradub, S. Soft bio-composites from natural rubber (NR) and marine products. In *Chemistry, Manufacture and Applications of Natural Rubber*; Elsevier: Amsterdam, The Netherlands, 2014; pp. 303–324. [CrossRef]
98. Alemdar, A.; Sain, M. Isolation and characterization of nanofibers from agricultural residues—Wheat straw and soy hulls. *Bioresour. Technol.* **2008**, *99*, 1664–1671. [CrossRef]
99. Neto, W.P.F.; Silvério, H.A.; Dantas, N.O.; Pasquini, D. Extraction and characterization of cellulose nanocrystals from agro-industrial residue—Soy hulls. *Ind. Crops Prod.* **2013**, *42*, 480–488. [CrossRef]
100. Kolattukudy, P.E. Biopolyester membranes of plants: Cutin and suberin. *Science* **1980**, *208*, 990–1000. [CrossRef]
101. Wang, Y.; Li, X.; Sun, G.; Li, D.; Pan, Z. A comparison of dynamic mechanical properties of processing-tomato peel as affected by hot lye and infrared radiation heating for peeling. *J. Food Eng.* **2014**, *126*, 27–34. [CrossRef]
102. Mwaikambo, L.Y.; Ansell, M.P. Chemical modification of hemp, sisal, jute, and kapok fibers by alkalization. *J. Appl. Polym. Sci.* **2002**, *84*, 2222–2234. [CrossRef]
103. George, N.; Chandra, J.; Mathiazhagan, A.; Joseph, R. High performance natural rubber composites with conductive segregated network of multiwalled carbon nanotubes. *Compos. Sci. Technol.* **2015**, *116*, 33–40. [CrossRef]
104. Hao, D.; Shou-ci, L.; Yan-xi, D.; Gao-xiang, D. Mechano-activated surface modification of calcium carbonate in wet stirred mill. *Trans. Nonferrous. Met. Soc. China.* **2007**, *17*, 1100–1104.
105. Faix, O. Fourier Transform Infrared Spectroscopy. In *Methods in Lignin Chemistry*; Springer: Berlin/Heidelberg, Germany, 1992; pp. 83–109. [CrossRef]
106. Mayers, J.J.; Flynn, K.J.; Shields, R.J. Rapid determination of bulk microalgal biochemical composition by Fourier-Transform Infrared spectroscopy. *Bioresour. Technol.* **2013**, *148*, 215–220. [CrossRef]
107. Barrios, V.; Méndez, J.; Aguilar, N. FTIR–An Essential Characterization Technique for Polymeric Materials, Cdn. Intechopen. Com. 2003. Available online: http://cdn.intechopen.com/pdfs/36174/InTech-Ftir_an_essential_characterization_technique_for_polymeric_materials.pdf (accessed on 19 September 2019).
108. Knutson, K.; Lyman, D.J. Surface Infrared Spectroscopy. In *Surface and Interfacial Aspects of Biomedical Polymers*; Springer: Boston, MA, USA, 1985; pp. 197–247. [CrossRef]
109. Sgriccia, N.; Hawley, M.C.; Misra, M. Characterization of natural fiber surfaces and natural fiber composites. *Compos. Part A Appl. Sci. Manuf.* **2008**, *39*, 1632–1637. [CrossRef]
110. Grady, B.P.; Cooper, S.L.; Robertson, C.G. Thermoplastic Elastomers. In *The Science and Technology of Rubber*; Elsevier: Amsterdam, The Netherlands, 2013; pp. 591–652. [CrossRef]
111. Fombuena, V.; Bernardi, L.; Fenollar, O.; Boronat, T.; Balart, R. Characterization of green composites from biobased epoxy matrices and bio-fillers derived from seashell wastes. *J. Mater.* **2014**, *57*, 168–174. [CrossRef]
112. Bello, M.O.; Abdus-Salam, N.; Adekola, F.A. Utilization of Guinea corn (Sughurm vulgare) Husk for Preparation of Bio-based Silica and its Characterization Studies. *Int. J. Environ. Agric. Biotechnol.* **2018**, *3*, 670–675. [CrossRef]

113. Kibel, M.H. X-Ray Photoelectron Spectroscopy. In *Surface Analysis Methods in Materials Science*; O'Connor, D.J., Sexton, B.A., Smart, R.S.C., Eds.; Springer: Berlin/Heidelberg, Germany, 2003; pp. 175–201. [CrossRef]
114. Mettler-Toledo GmbH Analytical, Thermal Analysis Information for Users—User Com 45, Thermogravimetry and Gas Analysis, Part 1: Basic Principles and Overview (2017). Available online: https://www.mt.com/us/en/home/library/usercoms/lab-analytical-instruments/thermal-analysis-usercom-45.html (accessed on 12 November 2019).
115. Mettler-Toledo GmbH Analytical, Thermal Analysis Information for Users—User Com 47, Thermogravimetry and Gas Analysis, Part 3: TGA/DSC-FTIR (2018). Available online: https://www.mt.com/us/en/home/library/usercoms/lab-analytical-instruments/thermal-analysis-usercom-47.html (accessed on 12 November 2019).
116. Li, S.; Lyons-Hart, J.; Banyasz, J.; Shafer, K. Real-time evolved gas analysis by FTIR method: An experimental study of cellulose pyrolysis. *Fuel* **2001**, *80*, 1809–1817. [CrossRef]
117. Bitinis, N.; Verdejo, R.; Bras, J.; Fortunati, E.; Kenny, J.M.; Torre, L. Poly(lactic acid)/natural rubber/cellulose nanocrystal bionanocomposites Part, I. Processing and morphology. *Carbohydr. Polym.* **2013**, *96*, 611–620. [CrossRef]
118. Xie, W.; Pan, W.P. Thermal characterization of materials using evolved gas analysis. *J. Therm. Anal. Calorim.* **2001**, *65*, 669–685. [CrossRef]
119. Kim, H.-Y.; Park, S.S.; Lim, S.-T. Preparation, characterization and utilization of starch nanoparticles. *Colloids Surf. B Biointerfaces* **2015**, *126*, 607–620. [CrossRef]
120. Conzatti, L.; Galimberti, M. Microscopy of Natural Rubber Composites and Nanocomposites. In *Natural Rubber Materials*; Thomas, S., Chan, C.H., Pothen, L., Joy, J., Maria, H., Eds.; The Royal Society of Chemistry: London, UK, 2014; Volume 2, pp. 649–682. [CrossRef]
121. Visakh, P.M.; Thomas, S.; Oksman, K.; Mathew, A.P. Crosslinked natural rubber nanocomposites reinforced with cellulose whiskers isolated from bamboo waste: Processing and mechanical/thermal properties. *Compos. Part A Appl. Sci. Manuf.* **2012**, *43*, 735–741. [CrossRef]
122. Turner, P.S.; Nockolds, C.E.; Bulcock, S. Electron Microscope Techniques for Surface Characterization. In *Surface Analysis Methods in Materials Science*; O'connor, D.J., Sexton, B.A., Smart, R.S.C., Eds.; Springer: Berlin/Heidelberg, Germany, 2003; pp. 85–105. [CrossRef]
123. Karimi, K.; Taherzadeh, M.J. A critical review of analytical methods in pretreatment of lignocelluloses: Composition, imaging, and crystallinity. *Bioresour. Technol.* **2016**, *200*, 1008–1018. [CrossRef] [PubMed]
124. Kohjiya, S.; Katoh, A.; Suda, T.; Shimanuki, J.; Ikeda, Y. Visualisation of carbon black networks in rubbery matrix by skeletonisation of 3D-TEM image. *Polymer* **2006**, *47*, 3298–3301. [CrossRef]
125. Rebouillat, S.; Pla, F. State of the Art Manufacturing and Engineering of Nanocellulose: A Review of Available Data and Industrial Applications. *J. Biomater. Nanobiotechnol.* **2013**, *4*, 165–188. [CrossRef]
126. Bras, J.; Viet, D.; Bruzzese, C.; Dufresne, A. Correlation between stiffness of sheets prepared from cellulose whiskers and nanoparticles dimensions. *Carbohydr. Polym.* **2011**, *84*, 211–215. [CrossRef]
127. Bras, J.; Hassan, M.L.; Bruzesse, C.; Hassan, E.A.; El-Wakil, N.A.; Dufresne, A. Mechanical, barrier, and biodegradability properties of bagasse cellulose whiskers reinforced natural rubber nanocomposites. *Ind. Crops Prod.* **2010**, *32*, 627–633. [CrossRef]
128. Nunes, C.; Mahendrasingam, A.; Suryanarayanan, R. Quantification of crystallinity in substantially amorphous materials by synchrotron X-ray powder diffractometry. *Pharm. Res.* **2005**, *22*, 1942–1953. [CrossRef]
129. Visakh, P.M.; Thomas, S. Preparation of bionanomaterials and their polymer nanocomposites from waste and biomass. *Waste Biomass Valorization* **2010**, *1*, 121–134. [CrossRef]
130. Abdou, E.S.; Nagy, K.S.A.; Elsabee, M.Z. Extraction and characterization of chitin and chitosan from local sources. *Bioresour. Technol.* **2008**, *99*, 1359–1367. [CrossRef]
131. Filho, G.R.; de Assunção, R.M.N.; Vieira, J.G.; Meireles, C.D.; Cerqueira, D.A.; Barud, H.D. Characterization of methylcellulose produced from sugar cane bagasse cellulose: Crystallinity and thermal properties. *Polym. Degrad. Stab.* **2007**, *92*, 205–210. [CrossRef]
132. Cao, J.; Billows, C.A. Crystallinity determination of native and stretched wool by X-ray diffraction. *Polym. Int.* **1999**, *48*, 1027–1033. [CrossRef]
133. Park, S.; Baker, J.O.; Himmel, M.E.; Parilla, P.A.; Johnson, D.K. Cellulose crystallinity index: Measurement techniques and their impact on interpreting cellulase performance. *Biotechnol. Biofuels* **2010**, *3*, 10. [CrossRef]

134. Segal, L.; Creely, J.J.; Martin, A.E.; Conrad, C.M. An Empirical Method for Estimating the Degree of Crystallinity of Native Cellulose Using the X-Ray Diffractometer. *Text. Res. J.* **1958**, *29*, 786–794. [CrossRef]
135. Jiang, F.; Hsieh, Y.-L. Cellulose nanocrystal isolation from tomato peels and assembled nanofibers. *Carbohydr. Polym.* **2015**, *122*, 60–68. [CrossRef]